Journal of Engineering Mechanics. Submitted April 23, 2013; accepted December 2, 2013;
posted ahead of print December 4, 2013. doi:10.1061/(ASCE)EM.1943-7889.0000759

Nonlinear Joint Model Updating in Assembled Structures

Mehrisadat Makki Alamdari [1], Jianchun Li [2], Bijan Samali [3], Hamid Ahmadian [4], Ali Naghavi[5]

ABSTRACT

Dynamic response of mechanical structures is significantly affected by joints. Joints introduce remarkable frictional damping and localized flexibility to the structure; hence, to get a more accurate representation of a system dynamics, it is crucial to take into account these effects. This paper investigates the application of the finite element model updating on characterization of a nonlinear joint interface. A thin layer of virtual elements is used at joint location to represent the nonlinear behavior of the coupling in tangential direction. The material properties of the elements are described by nonlinear constitutive stress-strain equation which defines nonlinear state of the joint interface. In this study, Richard–Abbot Elastic-Plastic material was considered, which is capable of characterizing energy dissipation and softening phenomena in joint at nonlinear state. Uncertain material parameters are adjusted to minimize the residual between the numerical and experimental nonlinear frequency responses. Minimization was carried out based on iterative sensitivity-based optimization. The procedure was implemented on an assembled structure consisting of two steel threaded pipes coupled to each other by a nut interface. It was demonstrated that the proposed technique significantly reduces the uncertainties in the joint modeling and leads to a more reliable description of the assembled structure.

Keywords*:* Component Mode Synthesis, Finite Element Model Updating, Mechanical Joint, Frequency Response Function (FRF).

Accepted Manuscript
Not Copyedited

[1] * Corresponding author.
E-mail addresses:mehri.makki@gmail.com
PhD student, Centre for Built Infrastructure Research (CBIR), School of Civil and Environmental Engineering, University of Technology Sydney, Ultimo, NSW, Australia.
[2] *E-mail addresses: Jianchun.Li@uts.edu.au*
Associated Professor, Centre for Built Infrastructure Research (CBIR), School of Civil and Environmental Engineering, University of Technology Sydney, Ultimo, NSW, Australia.
3 E-mail addresses: Bijan.Samali@uts.edu.au
Professor, Centre for Built Infrastructure Research (CBIR), School of Civil and Environmental Engineering, University of Technology Sydney, Ultimo, NSW, Australia.
[4] *E-mail addresses: Ahmadian@iust.ac.ir*
Professor, Centre of Excellence in Experimental Solid Mechanics and Dynamics, School of Mechanical Engineering, Iran University of Science and Technology, Narmak, Tehran, 16846, Iran.
[5] *E-mail addresses: naghavi.EFM@gmail.com*
M.Sc. student, Centre of Excellence in Experimental Solid Mechanics and Dynamics, School of Mechanical Engineering, Iran University of Science and Technology, Narmak, Tehran, 16846, Iran.

Copyright 2013 by the American Society of Civil Engineers

Downloaded from ascelibrary.org by University of Newcastle on 12/17/13. Copyright ASCE. For personal use only; all rights reserved.

Journal of Engineering Mechanics. Submitted April 23, 2013; accepted December 2, 2013;
posted ahead of print December 4, 2013. doi:10.1061/(ASCE)EM.1943-7889.0000759

Downloaded from ascelibrary.org by University of Newcastle on 12/17/13. Copyright ASCE. For personal use only; all rights reserved.

INTRODUCTION

Nowadays, finite element method is commonly used in various areas of engineering analysis. Many complex structures are composed of sub-structures and components connected by mechanical joints to each other. The quality of the finite element model is largely affected by how joints and couplings are defined in the models. Having a more realistic representation of a mechanical joint is necessary to get reliable results from different computational analysis, specifically dynamic analysis, in which the stiffness and damping values play a crucial role in the final results e.g. natural frequency and response level.

Mechanical joints, due to complicated and nonlinear nature, involve considerable uncertainty in the modeling process. Ibrahim and Pettit (2005) provided a review on different sources of uncertainty in mechanical fasteners. One of the main causes of this nonlinear and complex behavior is friction. Because of localized slippage over the contact interfaces, mechanical joint is undergoing frictional dissipation which can be correlated to damping. This phenomenon is non-smooth and introduces considerable nonlinearity to the system. In addition, the joint stiffness changes with excitation level. As excitation level increases, the natural frequency of the assembled structure reduces because of the increasing flexibility at joint location. Therefore, consideration of these uncertainties is vital to obtain proper characterization of mechanical joints.

Modeling of joints has been investigated by many researchers. Bograd et al. (2011) presented a paper on different approaches of joint modeling in assembled structures. In the context of finite element analysis, depending on the size of the joint, two categories can be defined: (i) lumped or nodal interface elements which have no spatial dimension, (0-D) and contain node-to-node spring and dashpot elements (ii) continuous interface elements which include (1-D) or (2-D) interface models, so-called thin layer or zero thickness elements. The second category is superior to the lumped model, since the three-dimensional behavior of contacting members can be modeled within one element. Moreover, the second approach makes possible to apply nonlinear stress-strain constitutive models to interface elements to represent the joint nonlinear hysteretic behavior.

Luan et al. (2012) used nodal interface elements by applying a rigid mass with two bi-linear springs to model mechanical properties of bolted flange joints in free damping condition. Mayer and Gaul

Accepted Manuscript
Not Copyedited

Copyright 2013 by the American Society of Civil Engineers

Journal of Engineering Mechanics. Submitted April 23, 2013; accepted December 2, 2013;
posted ahead of print December 4, 2013. doi:10.1061/(ASCE)EM.1943-7889.0000759

Downloaded from ascelibrary.org by University of Newcastle on 12/17/13. Copyright ASCE. For personal use only; all rights reserved.

(2007) provided an overview of (2-D) interface models and formulated thin layer and zero thickness interface elements. Ahmadian et al. (2002) applied a thin layer of solid elements with isotropic constitutive law to model linear behavior of face-to-face bolted flange connection between two pipes. Manzoli et al. (2012) used solid elements to model interfaces between components of composite structural members. The method was successfully applied to describe the bond degradation of steel bars in reinforced concrete members.

Basically, there are three states associated with a mechanical joint subject to increasing loading: stick, micro-slip and macro-slip. During the first state, mechanical joint exhibits completely linear and elastic behavior since there is no partial movement between contacting surfaces. With increasing force level, the normal pressure in the contact areas decreases; as a consequence, localized slip occurs in the interface while the most part of the joint is still in the stick. If the driving input load exeeds the threshold, the entire contact surfaces start to move relative to each other and the joint undergoes macro-slip. Transition from one state to another, alters interface stiffness and frictional dissipation which corresponds to the hysteresis mechanism. For a joint under sinusoidal periodic load, an elliptic hysteresis loop is expected during the stick state. By increasing frictional damping due to transition from stick to micro/ macro slip state, deviations appear in the hysteresis loop and results in nonlinear hysteresis behavior of a joint (Chen & Deng (2005), Adams & Nosonovsky (2000)).

Based on the previous research, it has been demonstrated that during micro-slip, the amplitude of vibration reduces as the level of excitation increases (Ahmadian (2007, 2009)). That is because energy dissipates through micro-slip at the joint. In contrast, by transition from micro/slip to macro-slip, an increasing trend in the response level will be observed. Magnevall et al. (2006) found that by increasing the force level and transition from micro-slip to macro-slip, the amplitude of response increases which is not the case for micro-slip. Therefore, it can be concluded that shifting the resonances to lower frequencies and initially a decreasing and then increasing trend in the vibration response are inevitable consequences of increasing the input energy in an assembled structure composed of mechanical joints.

The focus of the presented work is to develop a physical model to describe the joint behavior in an assembled structure under high level of excitation. The joint is under shear stress and transition from

Accepted Manuscript
Not Copyedited

Copyright 2013 by the American Society of Civil Engineers

Journal of Engineering Mechanics. Submitted April 23, 2013; accepted December 2, 2013;
posted ahead of print December 4, 2013. doi:10.1061/(ASCE)EM.1943-7889.0000759

Downloaded from ascelibrary.org by University of Newcastle on 12/17/13. Copyright ASCE. For personal use only; all rights reserved.

stick to micro-slip is investigated. The physical behavior of the joint interface in stick and micro-slip is represented by a thin layer of solid elements with nonlinear material behavior. A nonlinear Richard–Abbot constitutive model is adopted which obeys the constant hysteresis principle. The elastic part of the constitutive model characterizes the linear behavior of the joint at low excitation levels, while the plastic part describes energy dissipation and softening effects in the joint at higher levels of excitations. In order to reduce the size of the coupled system and save computational time, Component Mode Synthesis (CMS) technique is utilized. In this regard, dynamics of the assembled structure is described by its components' Ritz vectors.

This paper is organized as follows: first, a brief review on different friction models is presented, followed by describing Richard–Abbot constitutive model which has been utilized in this work. A detailed description of an experimental case study is provided, continued by finite element model of the assembled structure. The paper is then followed by identification of the joint uncertain parameters by employing CMS approach to increase the efficiency of identification process. The paper ends with concluding the work and giving some suggestions for future works.

JOINT INTERFACE MODELNG

Several friction models have been proposed to characterize the joint transition from stick to micro/macro-slip and represent hysteretic contact dissipation, Dahl (1976), Valanis (1971), Gaul & Lenz (1997). Masing (1926) developed a model, consisting of a collection of Jenkins elements, in parallel, to describe the hysteresis behavior of metals. Each Jenkins element consists of a linear spring with elastic stiffness in series with a Coulomb slider. According to this approach, a one-dimensional hysteretic system may be viewed as a collection of elastic-perfectly plastic elements as shown in Fig. 1 (a). The enclosed area in force-displacement curve indicates dissipated friction energy in the system. Masing model has been applied in the fields of friction contact modeling, Stanbridge et al. (1999), and material plasticity, Segal &Val (2000).

Figure 1. Force–deformation hysteresis loops, (a) single Jenkins model, (b) bilinear elastic-plastic model, (c) nonlinear elastic-plastic model.

Accepted Manuscript
Not Copyedited

Copyright 2013 by the American Society of Civil Engineers

Journal of Engineering Mechanics. Submitted April 23, 2013; accepted December 2, 2013;
posted ahead of print December 4, 2013. doi:10.1061/(ASCE)EM.1943-7889.0000759

Downloaded from ascelibrary.org by University of Newcastle on 12/17/13. Copyright ASCE. For personal use only; all rights reserved.

Accepted Manuscript
Not Copyedited

Bilinear elastic–plastic hysteresis model is another approach to simulate connection behavior; it has been successfully used by several researchers, Abad et al. (2012), Levy et al. (2001), Troup et al. (1998) and Romstad & Subramanian (1970). In situations that the hysteresis loop is close to bilinear model, it can be represented by one or two Jenkins elements. The bilinear model depends on three parameters: elastic stiffness, plastic stiffness and yielding point. Fig. 1 (b) indicates a typical force-deformation hysteresis loop corresponding to bilinear elastic-plastic model.

Nonlinear elastic-plastic model is the most accurate model to describe the joint behavior. Nonlinear model has an improved capability to describe stick, micro-slip, and macro-slip regions in a mechanical connection as depicted in Fig. 1 (c). Unlike the previous two models, this model offers smooth transition from stick to micro-slip and macro-slip. Ramberg and Osgood (1943) proposed a power-law relationship between force and plastic deformation. This model is able to describe the transition from stick to micro-slip and macro-slip by tuning shape factor parameter. Yee and Melchers (1986) proposed an exponential equation which allows positive, zero and negative plastic stiffness.

In this work, a nonlinear elastic-plastic model has been adopted to describe stick and micro slip mechanism of a mechanical interface subject to shear load. The general form of the constitutive equation for the interface element can be described by, (Mayer & Gaul (2007))

$$\begin{Bmatrix} \sigma_n \\ \tau_{Tx} \\ \tau_{Ty} \end{Bmatrix} = \begin{bmatrix} c_{11} & 0 & 0 \\ & c_{55} & 0 \\ Sym. & & c_{66} \end{bmatrix} \begin{Bmatrix} \varepsilon_n \\ \gamma_{Tx} \\ \gamma_{Ty} \end{Bmatrix} \qquad \text{Eq. 1}$$

where subscripts n, x and y, respectively, denote contact normal and local *x*- and *y*- tangential directions.

For a joint under low level of excitation, a linear behavior is expected which can be simulated by an isotropic material. In this situation, parameters c_{11} and $c_{55} = c_{66}$ will be, respectively, Young's modulus, E_n, and shear modulus, G_T, which define normal and tangential stiffness of the joint.

In our case, as presented later, by increasing the excitation amplitude, the mechanical connection undergoes nonlinear behavior which corresponds to softening effects in FRFs and frictional damping. In order to characterize these two phenomena, a nonlinear Richard–Abbot model has been adopted to

Copyright 2013 by the American Society of Civil Engineers

Journal of Engineering Mechanics. Submitted April 23, 2013; accepted December 2, 2013;
posted ahead of print December 4, 2013. doi:10.1061/(ASCE)EM.1943-7889.0000759

Downloaded from ascelibrary.org by University of Newcastle on 12/17/13. Copyright ASCE. For personal use only; all rights reserved.

describe stress-strain relationship in tangential direction. This model was first introduced by Richard & Abbott (1975) and was later used by several researchers, Richard et al. (1998) and Yim & Krauthammer (2012). The Richard–Abbot constitutive law can be described by the following equation,

$$\sigma = \frac{(E_e - E_p)\varepsilon}{\left\{1 + \left|\frac{(E_e - E_p)\varepsilon}{S_Y}\right|^n\right\}^{1/n}} + E_p\varepsilon \qquad \text{Eq. 2}$$

where E_e and E_p, respectively, describe sticking elastic stiffness and sliding plastic stiffness; S_Y, is defining the yield point and parameter n is the shape factor which adjusts the sharpness of the profile. Fig. 2, shows the stress-strain profiles for different shape factors. As seen, once $n = 0$, a conventional linear stress-strain curve will be obtained, $\sigma = E_e\varepsilon$. By increasing shape factor, the stress-strain curve tends to a smooth nonlinear profile, which is appropriate to describe the joint transition from stick to micro/macro slip, Fig. 1 (c). As the shape factor becomes larger, $n \to \infty$, the profile approaches to bilinear elastic-plastic model, (n=100). Hence, this model is capable of describing different states of a mechanical joint and predicting the force-displacement hysteresis loop. This model consists of four unknown parameters: E_e, E_p, S_Y, and n. These four unknown parameters are identified to match numerical and experimental results. The first parameter, E_e, mainly controls the slope of the stress-strain curve in the elastic part, stick, and therefore, will be identified using linear test results. On the other hand, the next three unknown parameters contribute to the nonlinear behavior of the joint interface, micro slip, thus, nonlinear test results will be employed in their identification process.

Accepted Manuscript
Not Copyedited

Figure 2. Nonlinear stress- strain constitutive law

EXPERIMENTAL INVESTIGATION

In order to demonstrate the viability of the proposed model in representing the joint behavior, an experimental case study was conducted. Test set up includes two unidentical steel threaded pipes

Copyright 2013 by the American Society of Civil Engineers

Journal of Engineering Mechanics. Submitted April 23, 2013; accepted December 2, 2013;
posted ahead of print December 4, 2013. doi:10.1061/(ASCE)EM.1943-7889.0000759

connected by a nut interface, as illustrated in Fig. 3. The length of the pipes are 1080 and 587 mm, with outer diameter of 114 mm and thickness of 3.8 mm. The coupling length is 85 mm with outer diameter of 122 mm and thickness 6 mm. In this investigation, the joint region is under shear load.

Figure 3. Experimental set up, (a) schematic of the assembled structure in clamped-free condition, (b) excitation of the structure at free end, (c) the interface between two pipes and location of two accelerometers.

The assembled structure is in the fixed-free condition; it was welded to a very stiff wall at one end and excited at the other end as depicted in Fig. 3 (a). A Brüel & Kjær electromagnetic shaker was used to generate the input force. To amplify the force signal, a power amplifier was placed in the circuit before the shaker. A sixteen-channel analyzer was used to process the data. Three kistler accelerometers were used to measure the dynamic response of the structure. Two accelerometers were placed fairly close to the coupling at both sides, as shown in Fig. 3 (c), and the third one was located close to the free end. The details of the test set up are presented in Fig. 4.

The set up was excited at two different conditions, (1) linear test, (2) nonlinear test; in the first experiment, the structure was excited with low amplitude pseudo random force, RMS 1 N. The frequency response of the structure was recorded in frequency range of (0-200 Hz) in terms of acceleration response. The measured frequency response function at free end is shown in Fig. 5. During this test, due to low level of excitation, the hysteresis function is considered to be in constant stick and therefore the assembled structure exhibits linear behavior; it can be observed by the obtained FRF with sharp peaks which correspond to a lightly damped system (there is no frictional damping at the joint interface). In addition, as it is visible, the peaks are symmetric with respect to resonance which is another indicator of a linear FRF (Jalali et al. (2011), Ahmadian and Jalai (2007)). According to this experiment, the first two bending natural frequencies are 28.5 Hz and 177 Hz , respectively.

Figure 4. The details of the test set up

Figure 5. Measured linear FRF at sensor location A_1

Accepted Manuscript
Not Copyedited

Downloaded from ascelibrary.org by University of Newcastle on 12/17/13. Copyright ASCE. For personal use only; all rights reserved.

Copyright 2013 by the American Society of Civil Engineers

Journal of Engineering Mechanics. Submitted April 23, 2013; accepted December 2, 2013;
posted ahead of print December 4, 2013. doi:10.1061/(ASCE)EM.1943-7889.0000759

Downloaded from ascelibrary.org by University of Newcastle on 12/17/13. Copyright ASCE. For personal use only; all rights reserved.

In the second experiment, the response of the structure is investigated at higher level of excitation by conducting step sine test. Despite being very slow, step sine test is the most accurate modal testing method which can provide high-quality information; specifically, in the case of nonlinear systems (Van der Auweraer et al. (1987)). The structure was excited by single harmonic sinusoidal force, RMS= 16.5 N, at selected discrete frequency points close to the first two resonances, one frequency at a time. The excitation amplitude was maintained at a constant level, 16.5 N, for all excitation frequencies. Fig. 6 (a) illustrates time history of the input force at different excitation frequencies. The steady state response of the structure was recorded at each excitation frequency as shown in Fig. 6 (b). It is worth mentioning that in the step sine test, it is necessary to ensure the steady-state condition is attained and the transient response must be negligible before the measurements are made. By employing amplitude ratios and phase shifts between the response and excitation, frequency responses are constructed point-by-point at each frequency step.

The nonlinear frequency responses at sensor location A_1, around the first and second modes, have been respectively, shown in Fig. 7 (a) and Fig. 7 (b).

As seen, by increasing excitation level, jump phenomenon occurs which is attributed to passage of the system from linear to nonlinear state, Carrella & Ewins (2011). Based on Fig. 7, there is a shifting in FRF peak; as a consequence, the first and second natural frequencies, respectively, reduce to 27.6 Hz and 175.7 Hz. A shift in natural frequency is an evident consequence of joint stiffness reduction. Another observation is that due to frictional dissipation initiating in the joint by increasing force level, the level of response decreases. Based on the presented results in Fig. 7, it can be concluded that in the second experiment, mechanical joint is undergoing micro-slip state which is associated with softening effect and damping increment. Therefore, in this study, the transition of mechanical joint from stick to micro-slip will be investigated. In this regard, measured linear and nonlinear FRFs will be employed to establish relevant uncertain parameters in the joint model.

Accepted Manuscript
Not Copyedited

Figure 6. Time history of the input excitation and output response, (a) single harmonic excitation at selected frequencies close to the first mode, (b) time history response of the structure at sensor location A_1.

Copyright 2013 by the American Society of Civil Engineers

Journal of Engineering Mechanics. Submitted April 23, 2013; accepted December 2, 2013;
posted ahead of print December 4, 2013. doi:10.1061/(ASCE)EM.1943-7889.0000759

Figure 7. Comparison between measured linear and nonlinear FRFs, (a) first bending mode, (b) second bending mode.

FINITE ELEMENT MODELING

The finite element model of the assembled structure was created in MD-NASTRAN; four-node shell elements (CQUAD4) were used to create the pipes and the mechanical interface between two pipes was created using a thin layer of eight-noded solid elements (CHEXA); totally, there are 56,000 degrees of freedom in the model to describe the dynamics of this assembled structure. See "Experimental investigation" for dimensions and details of the assembled structure. The FE model of the structure is shown in Fig. 8 (a) and Fig. 8 (b) which respectively, indicate the joint interface and the pipes.

Material property of the shell elements (pipes) is steel while nonlinear Richard–Abbot elastic-plastic material, Eq. 2, with unknown parameters which will be identified in the following sections, is considered for the interface elements.

In this work, to ensure the FE models of the substructures before assembling are reliable, each pipe in free support condition was separately excited using random vibration test within frequency band (0-1000 Hz). The FE model of each pipe was created in MD/NASTRAN and the numerical and experimental natural frequencies in the frequency band (0-1000 Hz) were compared. In order to match the numerical results and those obtained from the experiment, material properties of the steel were updated.

In order to obtain more accurate material properties (density and Young's moduli), the longer pipe, in free supported condition was investigated as depicted in Fig. 9. The first four flexible natural frequencies are numerically and experimentally obtained within frequency band (0-1000 Hz) as shown in Table 1; the least square error estimator, expressing the difference between the measured natural frequencies and the corresponding values of the numerical model was developed as follows,

$$Objective: \min \sum_{i=1}^{4} [(\omega_i^{FEM} - \omega_i^{Test}) / \omega_i^{Test}]^2 \qquad \text{Eq. 3}$$

Unknown material parameters in the numerical model were adjusted to minimize the residual using eigensensitivity analysis in MD/NASTRAN. It was found that the best values for the Young's

Accepted Manuscript Not Copyedited

Downloaded from ascelibrary.org by University of Newcastle on 12/17/13. Copyright ASCE. For personal use only; all rights reserved.

Copyright 2013 by the American Society of Civil Engineers

Journal of Engineering Mechanics. Submitted April 23, 2013; accepted December 2, 2013;
posted ahead of print December 4, 2013. doi:10.1061/(ASCE)EM.1943-7889.0000759

modulus and density will be respectively, 215 GPa and 7800 Kg/m^3 to minimize the residual. The obtained values are used in the subsequent analysis of the assembled structure in the finite element model.

Figure 8. Finite element model, (a) joint interface using solid elements, (b) pipes using shell elements.

Figure 9. Free-free vibration test on pipe with length 1080 mm

APPLICATION OF COMPONENT MODE SYNTHESIS (CMS)

Due to material nonlinearity at joint interface in the finite element model, the behavior of the assembled structure is nonlinear. Because of this nonlinearity, it is not possible to use traditional frequency methods to directly obtain FRFs; instead, for each excitation frequency, nonlinear transient analysis must be conducted to obtain transient response of the structure and consequently according to the steady state response of the structure, FRFs will be generated point by point. This algorithm is very time consuming and inefficient for a structure with high level of complexity specifically if the time step is considerably small. Moreover, in this work, uncertain material properties of the joint interface must be identified using optimization method. This means a large number of nonlinear transient analyses should be carried out for each iteration, depending on frequency resolution, to obtain FRFs for that iteration. Hence, the combination of structural nonlinearity and iterative optimization lead to huge computational time which can be significantly reduced by applying component mode synthesis approach (CMS).

Table 1. First four measured natural frequencies (Hz) of the longer pipe in separated free-supported condition.

CMS is a well-established method for efficiently constructing models to analyze the dynamics of large and complex structures. In this regard, the structure is decomposed into several components (substructures) and the response of the assembled structure is approximated by a set of vectors, where the number of vectors is considerably smaller than the number of physical degrees of freedom.

In this study, the assembled structure is decomposed into three substructures: pipes are considered as two substructures and the joint interface is defined as a residual structure. As there is no source of

Accepted Manuscript
Not Copyedited

Downloaded from ascelibrary.org by University of Newcastle on 12/17/13. Copyright ASCE. For personal use only; all rights reserved.

Copyright 2013 by the American Society of Civil Engineers

Journal of Engineering Mechanics. Submitted April 23, 2013; accepted December 2, 2013;
posted ahead of print December 4, 2013. doi:10.1061/(ASCE)EM.1943-7889.0000759

Downloaded from ascelibrary.org by University of Newcastle on 12/17/13. Copyright ASCE. For personal use only; all rights reserved.

nonlinearity in the pipes, it is possible to reduce their degrees of freedom before assembling them to residual structure. The dynamics of each sub-structure can be represented by,

$$\begin{bmatrix} M_{ii} & M_{ib} \\ M_{bi} & M_{bb} \end{bmatrix} \begin{Bmatrix} \ddot{u}_i \\ \ddot{u}_b \end{Bmatrix} + \begin{bmatrix} K_{ii} & K_{ib} \\ K_{bi} & K_{bb} \end{bmatrix} \begin{Bmatrix} u_i \\ u_b \end{Bmatrix} = \begin{Bmatrix} 0_i \\ f_b + r_b \end{Bmatrix} \quad \text{Eq. 4}$$

where M and K represent mass and stiffness of the substructure, partitioned based on internal, (subscript *(i)*) and boundary, (subscript *(b)*) degrees of freedom. f_b and r_b , respectively, describe the external and reaction forces at degrees of freedom located at interfaces between substructures.

In this work, Craig-Bampton CMS method is applied to reduce each pipe to its Ritz vectors. This reduction can be expressed by transformation of substructure matrices to a reduced domain as follows,

$$[M^{(s)},\ K^{(s)},\ f^{(s)},\ r^{(s)}] = \psi^{(s)T}[M,\ K,\ f,\ r]\ \psi^{(s)} \quad \text{Eq. 5}$$

where $\psi^{(s)}$ denotes transformation matrix and can be represented by,

$$\psi^{(s)} = [\varphi_{N_K}\ \ \psi_c] \quad \text{Eq. 6}$$

where φ_{N_K} and ψ_C are fixed-interface normal modes and constraint modes, respectively, for each substructure (Craig, (1968), (1987)).

MD/NASTRAN super-element module was employed to condense each pipe to its ortho-normal Ritz vectors by this transformation matrix. The joint interface is defined as a residual structure with no dynamic reduction. During the assembly run, the reduced external components are attached to the residual structure (Robinson, (2006)).

The effect of transformation matrix size (number of kept modes in Eq. 6) on processing time and accuracy of the response was investigated by conducting nonlinear transient analysis on the assembled structure. The Richard-Abbot parameters used for this simulation are as follows: $E_p = 1e6 Pa$, $S_Y = 1e6\ Pa$, and $n = 5$; the elastic modulus of the pipes and the joint interface are, respectively, 2.15e11 Pa and 7.00e10 Pa. The structure was excited using a single harmonic load at frequency of 20 Hz at free end and the steady state response was extracted at the same position. This investigation was carried out for three different cases: (i) No reduction, (ii) considering 5 Ritz vectors and (iii)

Accepted Manuscript
Not Copyedited

Copyright 2013 by the American Society of Civil Engineers

Journal of Engineering Mechanics. Submitted April 23, 2013; accepted December 2, 2013;
posted ahead of print December 4, 2013. doi:10.1061/(ASCE)EM.1943-7889.0000759

considering 30 Ritz vectors. The results are tabulated in Table 2. According to this table, with no dynamic reduction, the processing time is almost 2.7 times greater than those for the system represented by just five modes. Nevertheless, the condensed system is in a good agreement with the original model with no considerable penalty in the results' accuracy. Based on this observation, application of CMS not only improves the computational efficiency but also offers appropriate accuracy and thus is utilized in this work.

Table 2. Comparison of the responses between the condensed system and the original one

IDENTIFICATION OF JOINT UNCERTAIN PARAMETERS

As described in section "Joint Interface Modeling", there are totally four unknown parameters in the constitutive law which should be identified according to the measured FRFs from linear and nonlinear tests.

Once the excitation level is low, the joint interface is in complete stick condition and there is no localized slippage over the contact interface to introduce nonlinearity; thus, the structure exhibits linear behavior. Basically, in this situation, the response of the structure is controlled by only one parameter, Young's modulus. Therefore, it is acceptable to use linear test results to identify this uncertain parameter. In this regard, Young's modulus of thin layer interface elements is adjusted in a way to minimize the difference between the measured and predicted natural frequencies as follows,

$$Objective: \min \sum_{i=1}^{2} [(\omega_i^{FEM} - \omega_i^{Test}) / \omega_i^{Test}]^2 \quad \text{Eq. 7}$$

where ω denotes natural frequency of the assembled structure.

The identification procedure was performed using the design optimization module available in MD/NASTRAN. The design sensitivity procedure in MD/NASTRAN, which is elaborated by Muira (1988), is based on an iterative linear Eigen-sensitivity method using the following expression,

$$\Delta\lambda_n = \frac{\{\varphi_n\}^T (\Delta K - \lambda_n \Delta M)\{\varphi_n\}}{\{\varphi_n\}^T [M]\{\varphi_n\}} \quad \text{Eq. 8}$$

where $\Delta\lambda_n$ represents the perturbation in *n-th* eigenvalue.

Copyright 2013 by the American Society of Civil Engineers

Downloaded from ascelibrary.org by University of Newcastle on 12/17/13. Copyright ASCE. For personal use only; all rights reserved.

Accepted Manuscript Not Copyedited

Journal of Engineering Mechanics. Submitted April 23, 2013; accepted December 2, 2013;
posted ahead of print December 4, 2013. doi:10.1061/(ASCE)EM.1943-7889.0000759

Downloaded from ascelibrary.org by University of Newcastle on 12/17/13. Copyright ASCE. For personal use only; all rights reserved.

The choice of initial parameter was made as steel elastic modulus which was identified earlier (215 GPa). A permissible range of variation was also defined; the upper bound for the variation of the design variable was set to 1.1 of the initial value and the lower bound was set to 1e-5 of the initial value. The variation of design parameter during optimization is shown in Fig. 10. According to this figure, the stiffness of the interface decreases and after 8 iterations the design parameter converges to 70 GPa which is about 0.3 of the elastic modulus of the parent material. This observation demonstrates that even at low level of excitation, the joint stiffness might be much less than the stiffness of the parent material. The first two natural frequencies before and after updating are shown in Table 3. This table indicates the error between the first two natural frequencies obtained by initial FE model (before updating) and corresponding values obtained by linear test; as expected, prediction of the initial model is erroneous with about 15% error. However, by using this approach, the updated model is consistent with the measured data.

Figure 10. The convergence history of design parameter

Table 3. Comparison between the measured and predicted natural frequencies before and after updating (Hz)

In order to match the linear FRFs obtained via simulation and experiment, material damping has been introduced and applied to the elements belonging to the pipes. This damping corresponds to the pipes and not frictional contact interface. Material damping in MD/NASTRAN can be described on material property card.

To obtain linear FRFs in NASTRAN, frequency response analysis was conducted in frequency range (10-40 Hz), for the first mode, and (145-200 Hz), for the second mode, with frequency increment 0.1 Hz. Fig. 11 (a) and Fig.11 (b) respectively, compare updated and experimentally measured linear FRFs in terms of acceleration response. It can be seen that the linear updated results are in excellent agreement with FE model predictions and the test results.

Figure 11. Measured and updated linear FRFs around the (a) first mode, (b) second mode.

Accepted Manuscript
Not Copyedited

Copyright 2013 by the American Society of Civil Engineers

Journal of Engineering Mechanics. Submitted April 23, 2013; accepted December 2, 2013;
posted ahead of print December 4, 2013. doi:10.1061/(ASCE)EM.1943-7889.0000759

Downloaded from ascelibrary.org by University of Newcastle on 12/17/13. Copyright ASCE. For personal use only; all rights reserved.

So far, only one parameter of the joint model, E_e, describing its linear behavior, has been identified. Next, the nonlinear behavior of the test structure is utilized to identify the remaining uncertain parameters.

As mentioned earlier, localized flexibility and frictional damping are two inevitable consequences of a joint interface under high level of excitation. Unlike the linear test, where frictional damping at joint interface was inactive, during nonlinear test, due to slippage over the contact interfaces, friction plays a crucial role in the system behavior. The impact of this frictional dissipation is mostly related to response amplitude; hence, to consider both effects in identification procedure, nonlinear FRF data is the best candidate since it includes both resonance information and response amplitudes. Therefore, instead of using Eq. 7, which only contains information related to resonances, the following equation will be implemented to identify uncertain parameters.

$$OBJ : \min \sum_{i=1}^{m} [(\alpha^{FEM}(\omega_i) - \alpha^{Test}(\omega_i))/\alpha^{Test}(\omega_i)]^2 \quad \text{Eq. 9}$$
$$subject \quad to : E_p < E_e$$

where $\alpha(\omega)$ is nonlinear FRF in terms of acceleration at excitation frequency ω and m refers to the number of spectra.

In nonlinear test, the interface behavior is represented by nonlinear portion of the stress-strain curve, Eq. 2. There are three unknown parameters associated with this region: E_p, S_Y, and n; which will be identified to minimize the difference between the predicted and observed nonlinear FRFs according to Eq. 9.

In this work, FRF data around the first mode was applied to identify unknown parameters while FRF data around the second mode was employed to validate the identified system.

In order to numerically obtain $\alpha^{FEM}(\omega)$, the model was excited with a single harmonic load with amplitude of 16.5 N at frequency ω. Nonlinear transient analysis with simultaneous dynamic reduction approach (CMS) (considering 10 Ritz vectors) was utilized to obtain steady state response of the structure at free end in terms of acceleration. The ratio of the output amplitude to that of the input amplitude defines FRF at frequency ω.

Accepted Manuscript
Not Copyedited

Copyright 2013 by the American Society of Civil Engineers

Journal of Engineering Mechanics. Submitted April 23, 2013; accepted December 2, 2013;
posted ahead of print December 4, 2013. doi:10.1061/(ASCE)EM.1943-7889.0000759

A gradient-based Design Optimization Tool (DOT) is incorporated with MD/NASTRAN to solve this multi-variable implicit optimization problem subject to constraint shown in Eq. 9. The flowchart of the identification procedure is shown in Fig. 12.

Figure 12. The flowchart of the identification procedure using DOT

As depicted in Fig. 12, identification process starts with generating Nastran input file (.bdf) and is followed by running nonlinear transient analysis for *m* selected excitation frequencies around the first mode to generate the objective function, Eq. 9. The procedure continues with running DOT which takes current design parameters and corresponding objective values and modifies the design variables in search of the optimum by proposing new values for unknown parameters, E_p, S_Y, and n. The input file is updated based on new approximation for design variables and the procedure continues until the objective function is less than the predefined threshold value.

The convergence history is presented in Fig. 13. As shown, after 33 iterations, convergence occurs. Based on Fig. 13, it seems, S_Y has more impact on the system behavior and the error function is more sensitive to this parameter. The reason lies in the fact that S_Y controls the amount of damping in the structure. The lower S_Y means that the structure experiences plastic deformation with lower amount of input force; while higher S_Y indicates the need for more input force for the system to undergo plastic deformation. In contrast, E_p mostly deals with describing shifting phenomena and softening effects. The identified values for uncertain parameters are shown in Table 4.

Accepted Manuscript
Not Copyedited

Downloaded from ascelibrary.org by University of Newcastle on 12/17/13. Copyright ASCE. For personal use only; all rights reserved.

Copyright 2013 by the American Society of Civil Engineers

Journal of Engineering Mechanics. Submitted April 23, 2013; accepted December 2, 2013;
posted ahead of print December 4, 2013. doi:10.1061/(ASCE)EM.1943-7889.0000759

Figure 13. Convergence history of design parameters and objective

Table 4. Identification of parameters associated with nonlinear portion of the constitutive law

Having conducted the identification process, it is vital to verify the viability of the updated model in prediction of frequency responses around the second mode which have not been employed in the identification procedure. It is worth mentioning that the joint nonlinearity is displacement dependent and not frequency dependent as it involves friction. Basically, dissipation mechanism in the joint during the micro-slip depends solely on displacement amplitude; it has been demonstrated by several researchers that dissipation properties in the joint are frequency/velocity independent, Bograd et al (2011), Jalali et al (2007) and Hartwigsen et al (2004); therefore by showing the model predictions in other amplitudes, around the second mode, and matching the recorded response is enough to prove the validity of the identified model.

Hence, after obtaining uncertain parameters according to Table 4, nonlinear transient analysis was carried out at selected frequencies around the second mode to create FRFs. The results have been shown in Fig. 14. Fig. 14 (a) and Fig. 14 (b), respectively, show the FRFs around the first and second modes. As seen, the prediction of the updated model for frequency responses around the second mode is promising and the numerical results are in good agreement with those obtained via experiment. As illustrated in Fig. 14 (b) the level of response, which is substantially controlled by amount of damping, has been accurately estimated. It confirms that the proposed model is capable of characterizing the frictional dissipation in the joint interface. Furthermore, the prediction of the model for frequency shifting in FRF is consistent with observation; meaning, the proposed model is viable to represent the effects of localized flexibility occurring in the mechanical joints.

This investigation demonstrates that the proposed technique is suitable to improve the quality of joint modeling in finite element models by considering two major joint mechanisms: localized flexibility and frictional damping.

Figure 14. Comparison between FRFs obtained by FEM and experiment, (a) first mode, (b) second mode.

Accepted Manuscript
Not Copyedited

Downloaded from ascelibrary.org by University of Newcastle on 12/17/13. Copyright ASCE. For personal use only; all rights reserved.

Copyright 2013 by the American Society of Civil Engineers

Journal of Engineering Mechanics. Submitted April 23, 2013; accepted December 2, 2013;
posted ahead of print December 4, 2013. doi:10.1061/(ASCE)EM.1943-7889.0000759

Downloaded from ascelibrary.org by University of Newcastle on 12/17/13. Copyright ASCE. For personal use only; all rights reserved.

CONCLUSION

The aim of this article was to characterize the joint interface nonlinear behavior under high level of excitation. A thin layer of solid elements was utilized to model the joint interface between two pipes. A physical-based constitutive stress-strain law was adopted to simulate the joint behavior during stick and micro-slip regimes in tangential direction. The uncertain parameters were adjusted to minimize the residual between the measured and simulated frequency response functions. It was demonstrated that the method is capable of representing the joint behavior in stick and micro-slip regimes. Once the excitation level is low, the interface behavior is mostly represented by elastic part of the stress-strain law. On the other hand, by increasing the driving force and introducing nonlinearity to the system, the joint behavior is simulated by nonlinear and plastic part of the stress-strain curve. It was illustrated that this approach can accurately predict the softening effect and frictional damping in the joint. Application of this technique to discretization methods such as finite element method is beneficial as there is no limitation on constitutive law and any nonlinear form of stress-strain curve can be implemented depending on the problem under study.

To reduce computational time and improve the efficiency of the identification algorithm, CMS approach was applied. It was observed that by reducing the size and complexity of the problem, considerable saving in computational time occurs. Hence, it can be concluded that the combination of the above two paradigms leads to a more realistic description of the assembled structure in an efficient way.

The authors would like to propose some suggestions for future works:

1. In this work, the joint interface was subject to shear loading with tangential stress. The extension of the method for more complex joints including both shear and normal stresses might be of interest.
2. In the presented work, the entire identification and verification procedures were conducted based on a single level excitation (RMS=16.5 N). It is worthwhile to investigate the performance of the method for different excitation levels, e.g. identification is performed by one specific excitation level and verification is examined by a different excitation level.

Accepted Manuscript
Not Copyedited

Copyright 2013 by the American Society of Civil Engineers

Journal of Engineering Mechanics. Submitted April 23, 2013; accepted December 2, 2013;
posted ahead of print December 4, 2013. doi:10.1061/(ASCE)EM.1943-7889.0000759

Downloaded from ascelibrary.org by University of Newcastle on 12/17/13. Copyright ASCE. For personal use only; all rights reserved.

REFRENCES

1. Abad, J., Franco, J. M., Celorrio, R., & Lezáun, L. (2012). Design of experiments and energy dissipation analysis for a contact mechanics 3D model of frictional bolted lap joints. Advances in Engineering Software, 45(1), 42-53.
2. Adams, G. G., & Nosonovsky, M. (2000). Contact modelling — forces. Tribology International, 33(5–6), 431-442.
3. Ahmadian, H., Ebrahimi, M., Mottershead, J.E., Friswell, M.I. (2002). Identification of Bolted Joint Interface Models. ISMA 27, Leuven, Belgium, pp. 1741–1747.
4. Ahmadian, H., & Jalali, H. (2007). Generic element formulation for modelling bolted lap joints. Mechanical Systems and Signal Processing, 21(5), 2318-2334.
5. Ahmadian, H., & Zamani, A. (2009). Identification of nonlinear boundary effects using nonlinear normal modes. Mechanical Systems and Signal Processing, 23(6), 2008-2018.
6. Bograd, S., Reuss, P., Schmidt, A., Gaul, L., & Mayer, M. (2011). Modeling the dynamics of mechanical joints. Mechanical Systems and Signal Processing, 25(8), 2801-2826.
7. Carrella, A., & Ewins, D. J. (2011). Identifying and quantifying structural nonlinearities in engineering applications from measured frequency response functions. Mechanical Systems and Signal Processing, 25(3), 1011-1027.
8. Chen, W., & Deng, X. (2005). Structural damping caused by micro-slip along frictional interfaces. International Journal of Mechanical Sciences, 47(8), 1191-1211.
9. Craig, R.R., and Bampton. M. C. C., (1968), Coupling of Sub-structures for Dynamic Analysis, AIAA Journal, 6 (7), 1313-1319.
10. Craig Jr. RR. (1987), A review of time-domain and frequency domain component mode synthesis method, International Journal of Analytical and Experimental Modal Analysis, 2(2), 59-72.
11. Craig, R.R., Coupling of sub-structures for dynamic analyses: an overview, in: Structures, Structural Dynamics and Material Conference, 41st AIAA/ ASME/ ASCE/ AHS/ASC, Atlanta, 2000, AIAA-2000-1573.
12. Dahl, P.R. (1976). Solid friction damping of mechanical vibrations, AIAA Journal 14, 1675–1682. 25
13. Gaul L., Lenz, J., (1997) Nonlinear dynamics of structures assembled by bolted joints, Acta Mechanica 125, 169–181.

Accepted Manuscript
Not Copyedited

Copyright 2013 by the American Society of Civil Engineers

Journal of Engineering Mechanics. Submitted April 23, 2013; accepted December 2, 2013;
posted ahead of print December 4, 2013. doi:10.1061/(ASCE)EM.1943-7889.0000759

Downloaded from ascelibrary.org by University of Newcastle on 12/17/13. Copyright ASCE. For personal use only; all rights reserved.

14. Hartwigsen, C.J., Song, Y., McFarland, D.M., Bergman, L.A., Vakakis, A.F., 2004. Experimental study of non-linear effects in a typical shear lap joint configuration. Journal of Sound and Vibration 277 (1–2), 327–351.
15. Ibrahim, R. A., & Pettit, C. L. (2005). Uncertainties and dynamic problems of bolted joints and other fasteners. Journal of Sound and Vibration, 279(3–5), 857-936.
16. Jalali, H., Ahmadian, H., & Mottershead, J. E. (2007). Identification of nonlinear bolted lap-joint parameters by force-state mapping. International Journal of Solids and Structures, 44(25–26), 8087-8105.
17. Jalali, H., Ahmadian, H., & Pourahmadian, F. (2011). Identification of micro-vibro-impacts at boundary condition of a nonlinear beam. Mechanical Systems and Signal Processing, 25(3), 1073-1085.
18. Luan, Y., Guan, Z., Cheng, G., & Liu, S. (2012). A simplified nonlinear dynamic model for the analysis of pipe structures with bolted flange joints. Journal of Sound and Vibration, 331(2), 325-344.
19. Levy, R., Marianchik, E., Rutenberg, A., & Segal, F. (2001). A simple approach to the seismic design of friction damped braced medium-rise frames. Engineering Structures, 23(3), 250-259.
20. Magnevall. M, Josefsson A., Ahlin K., (2006). Parameter Estimation of Hysteresis Elements Using Harmonic Input, Department of Mechanical Engineering, Blekinge Institute of Technology, Sweden.
21. Manzoli, O. L., Gamino, A. L., Rodrigues, E. A., & Claro, G. K. S. (2012). Modelling of interfaces in two-dimensional problems using solid finite elements with high aspect ratio. Computers & Structures, 94–95(0), 70-82.
22. Masing, G. (1926). Self-stretching and hardening for brass, in: Proceedings of the 2nd International Congress for Applied Mechanics, pp. 332–335.
23. Mayer, M. H., & Gaul, L. (2007). Segment-to-segment contact elements for modelling joint interfaces in finite element analysis. Mechanical Systems and Signal Processing, 21(2), 724-734.
24. MUIRA, H. 1988. MSC/NASTRAN Handbook for Structural Optimization, The MacNeal-Schwendler Corporation.
25. Ramberg W, Osgood WR. Description of stress–strain curves by three parameters. National Advisory Committee for Aeronautics, Technical report 902; 1943.
26. Richard, R.M., Hisa, W.K. and Chrnielowiec, M. ‘‘Derived moment–rotation curves for double framing angles’’, Journal of Computers & Structures, 30(3), pp. 485–494 (1998).

Accepted Manuscript
Not Copyedited

Copyright 2013 by the American Society of Civil Engineers

Journal of Engineering Mechanics. Submitted April 23, 2013; accepted December 2, 2013;
posted ahead of print December 4, 2013. doi:10.1061/(ASCE)EM.1943-7889.0000759

27. Richard RM, Abbott BJ. Versatile elastic plastic stress–strain formula. J Eng Mech 1975;101(4):511–5.

28. Robinson, M., 2006, External Superelements in MSC. Nastran & MD Nastran.

29. Romstad KM, Subramanian CV. Analysis of frames with partial connection rigidity. Journal of Structural Division 1970; 96(ST11):228–300.

30. Segal, F., Val, D.V., (2000). Energy evaluation for Ramberg–Osgood hysteretic model, J. Eng. Mech. 132 (9) 907–913.

31. Stanbridge, A.B., Sanliturk, K.J., Ewins, D.J., (1999). Measurement and analysis of height–temperature friction damper properties, Proceedings of the Fourth National Turbine Engine High Cycle Fatigue (HCF) Conference.

32. Troup S, Xiao RY, Moy SSJ. Numerical modelling of bolted steel connections. Journal of Constructional Steel Research 1998; 46(1):269.

33. Van der Auweraer, H., Vanherck, P., Sas, P., & Snoeys, R. (1987). Accurate modal analysis measurements with programmed sine wave excitation. Mechanical Systems and Signal Processing, 1(3), 301-313.

34. Valanis, K.C. (1971). A theory of viscoplasticity without a yield surface, Archives of Mechanics 23 (4) 171–191.

35. Yee KL, Melchers RE. Moment–rotation curves for bolted connections. Journal of Structural Engineering 1986;112:615–35.

36. Yim, H. C., & Krauthammer, T. (2012). Mechanical properties of single-plate shear connections under monotonic, cyclic, and blast loads. Engineering Structures, 37(0), 24-35.

Downloaded from ascelibrary.org by University of Newcastle on 12/17/13. Copyright ASCE. For personal use only; all rights reserved.

Accepted Manuscript
Not Copyedited

Copyright 2013 by the American Society of Civil Engineers

Fig1.pdf

Journal of Engineering Mechanics. Submitted April 23, 2013; accepted December 2, 2013;
posted ahead of print December 4, 2013. doi:10.1061/(ASCE)EM.1943-7889.0000759

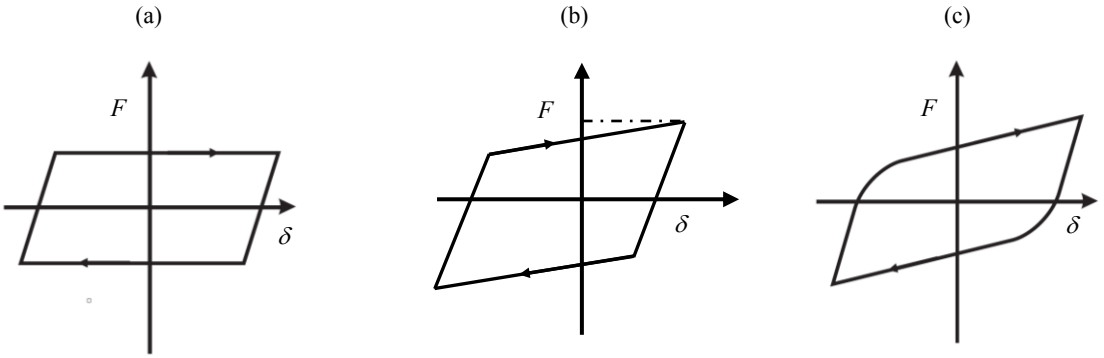

Downloaded from ascelibrary.org by University of Newcastle on 12/17/13. Copyright ASCE. For personal use only; all rights reserved.

Accepted Manuscript
Not Copyedited

Copyright 2013 by the American Society of Civil Engineers

Fig2.pdf

Journal of Engineering Mechanics. Submitted April 23, 2013; accepted December 2, 2013;
posted ahead of print December 4, 2013. doi:10.1061/(ASCE)EM.1943-7889.0000759

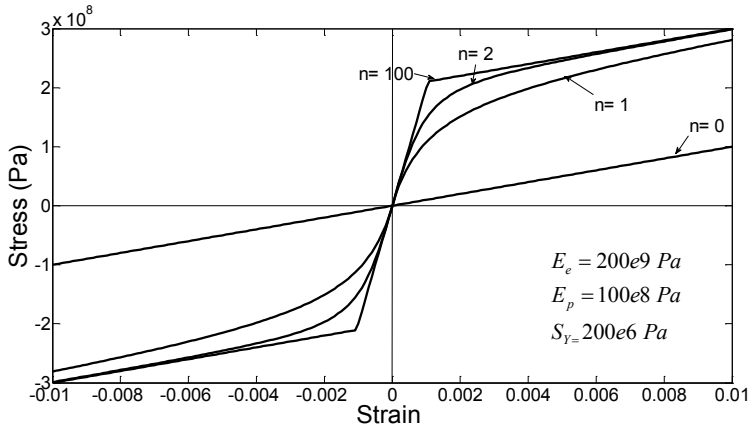

Downloaded from ascelibrary.org by University of Newcastle on 12/17/13. Copyright ASCE. For personal use only; all rights reserved.

Accepted Manuscript
Not Copyedited

Copyright 2013 by the American Society of Civil Engineers

Fig3_a.pdf

Journal of Engineering Mechanics. Submitted April 23, 2013; accepted December 2, 2013;
posted ahead of print December 4, 2013. doi:10.1061/(ASCE)EM.1943-7889.0000759

Downloaded from ascelibrary.org by University of Newcastle on 12/17/13. Copyright ASCE. For personal use only; all rights reserved.

Accepted Manuscript
Not Copyedited

Copyright 2013 by the American Society of Civil Engineers

Fig3_b.pdf

Journal of Engineering Mechanics. Submitted April 23, 2013; accepted December 2, 2013;
posted ahead of print December 4, 2013. doi:10.1061/(ASCE)EM.1943-7889.0000759

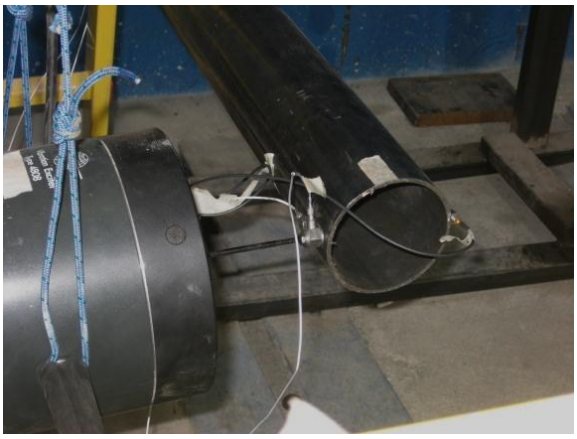

Downloaded from ascelibrary.org by University of Newcastle on 12/17/13. Copyright ASCE. For personal use only; all rights reserved.

Accepted Manuscript
Not Copyedited

Copyright 2013 by the American Society of Civil Engineers

Fig3_c.pdf

Journal of Engineering Mechanics. Submitted April 23, 2013; accepted December 2, 2013;
posted ahead of print December 4, 2013. doi:10.1061/(ASCE)EM.1943-7889.0000759

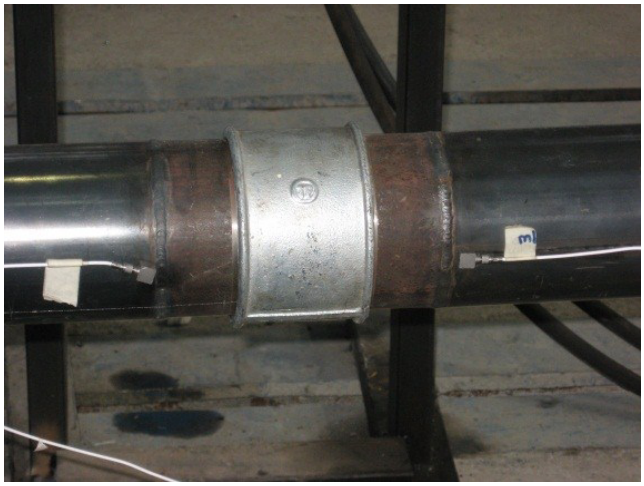

Downloaded from ascelibrary.org by University of Newcastle on 12/17/13. Copyright ASCE. For personal use only; all rights reserved.

Accepted Manuscript
Not Copyedited

Copyright 2013 by the American Society of Civil Engineers

Fig4.pdf

Journal of Engineering Mechanics. Submitted April 23, 2013; accepted December 2, 2013;
posted ahead of print December 4, 2013. doi:10.1061/(ASCE)EM.1943-7889.0000759

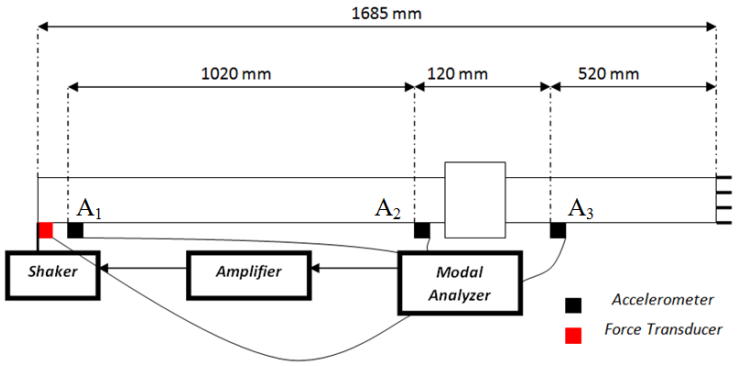

Downloaded from ascelibrary.org by University of Newcastle on 12/17/13. Copyright ASCE. For personal use only; all rights reserved.

Accepted Manuscript
Not Copyedited

Copyright 2013 by the American Society of Civil Engineers

Fig5.pdf

Journal of Engineering Mechanics. Submitted April 23, 2013; accepted December 2, 2013;
posted ahead of print December 4, 2013. doi:10.1061/(ASCE)EM.1943-7889.0000759

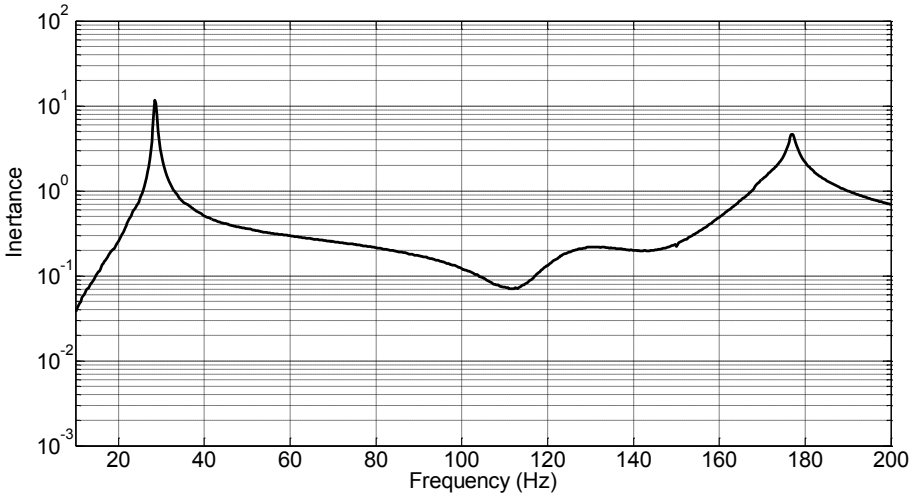

Downloaded from ascelibrary.org by University of Newcastle on 12/17/13. Copyright ASCE. For personal use only; all rights reserved.

Accepted Manuscript
Not Copyedited

Copyright 2013 by the American Society of Civil Engineers

Fig6_a.pdf

Journal of Engineering Mechanics. Submitted April 23, 2013; accepted December 2, 2013;
posted ahead of print December 4, 2013. doi:10.1061/(ASCE)EM.1943-7889.0000759

Downloaded from ascelibrary.org by University of Newcastle on 12/17/13. Copyright ASCE. For personal use only; all rights reserved.

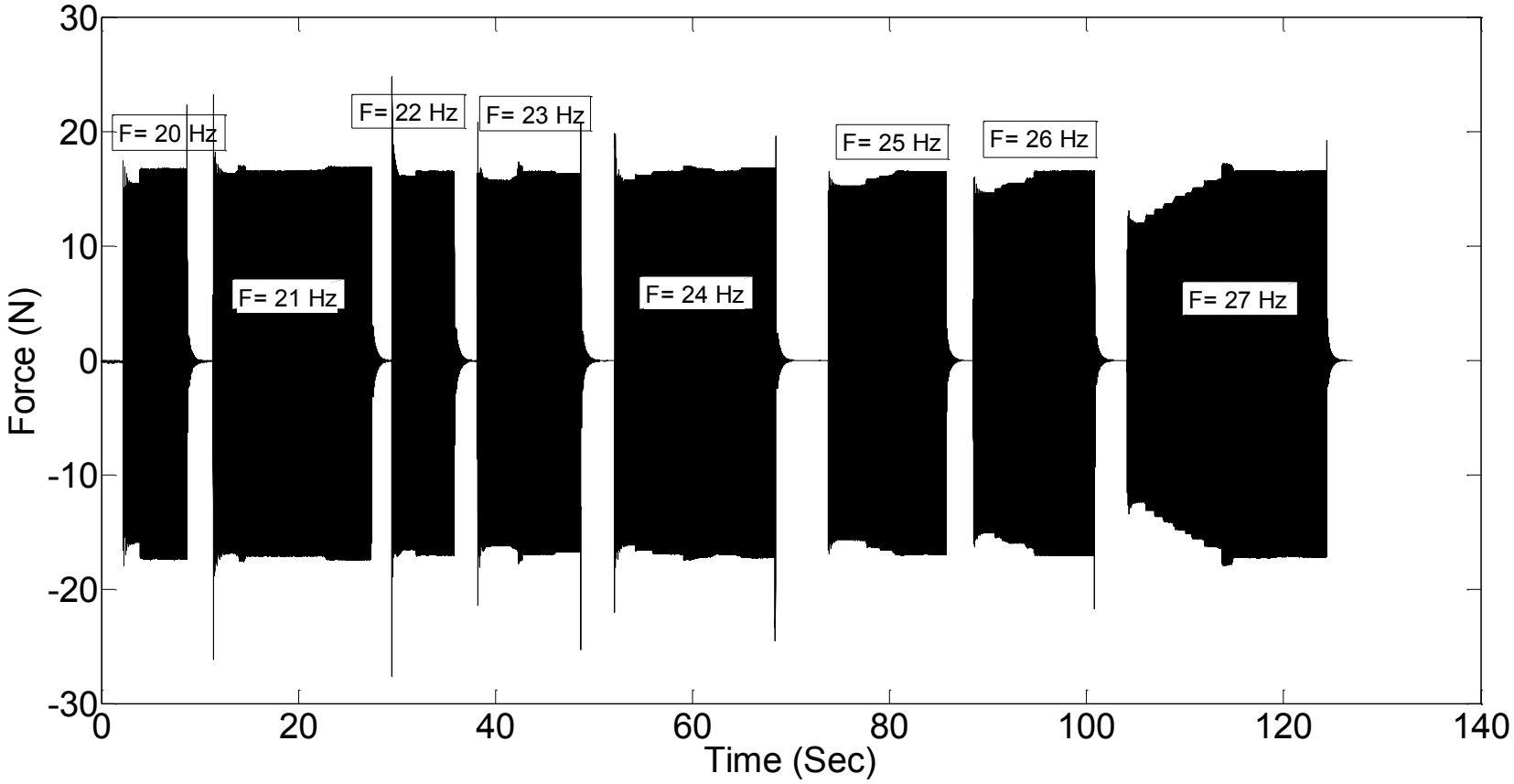

Accepted Manuscript
Not Copyedited

Copyright 2013 by the American Society of Civil Engineers

Fig6_b.pdf

Journal of Engineering Mechanics. Submitted April 23, 2013; accepted December 2, 2013;
posted ahead of print December 4, 2013. doi:10.1061/(ASCE)EM.1943-7889.0000759

Downloaded from ascelibrary.org by University of Newcastle on 12/17/13. Copyright ASCE. For personal use only; all rights reserved.

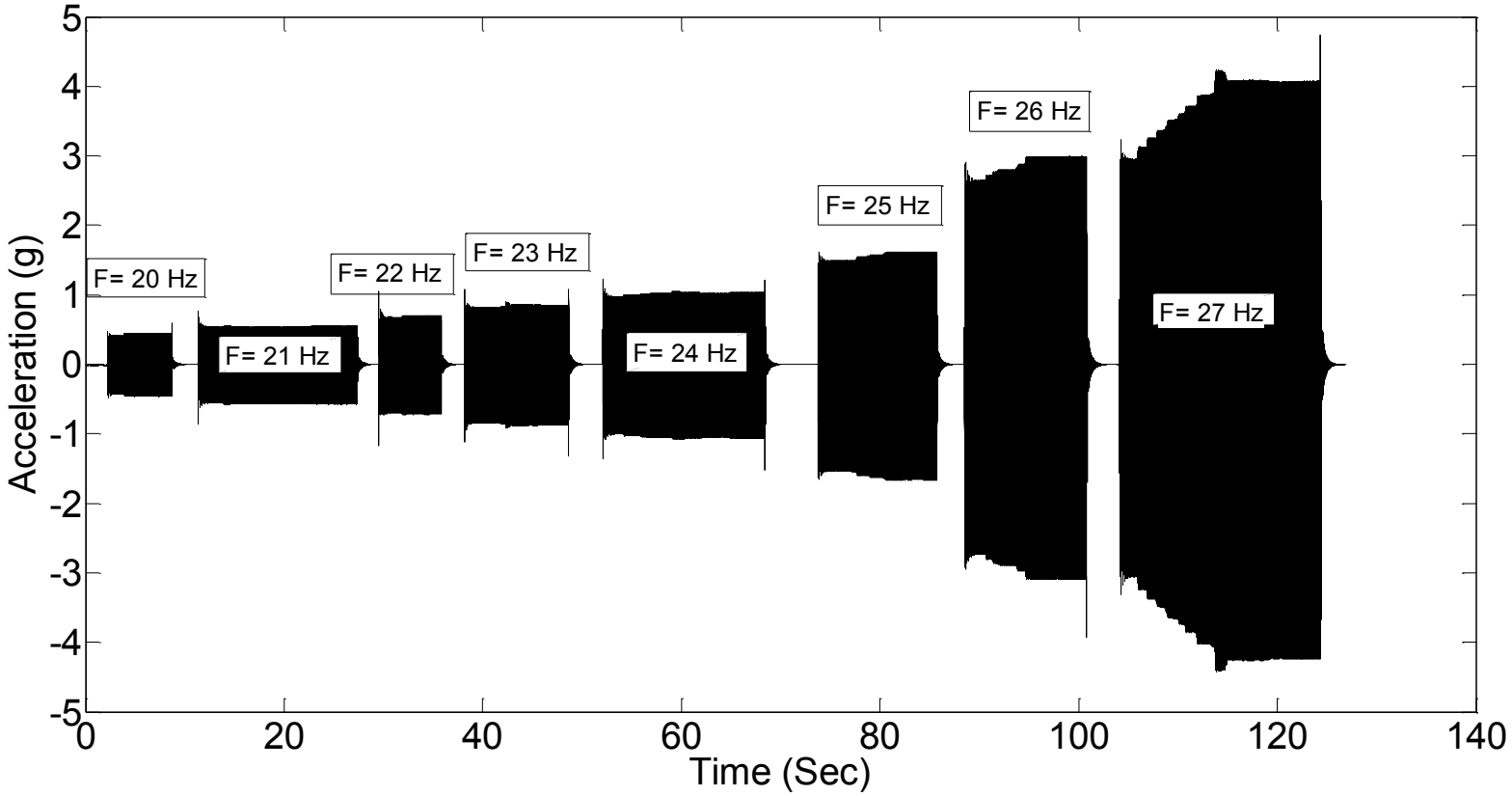

Accepted Manuscript
Not Copyedited

Copyright 2013 by the American Society of Civil Engineers

Fig7_a.pdf

Journal of Engineering Mechanics. Submitted April 23, 2013; accepted December 2, 2013;
posted ahead of print December 4, 2013. doi:10.1061/(ASCE)EM.1943-7889.0000759

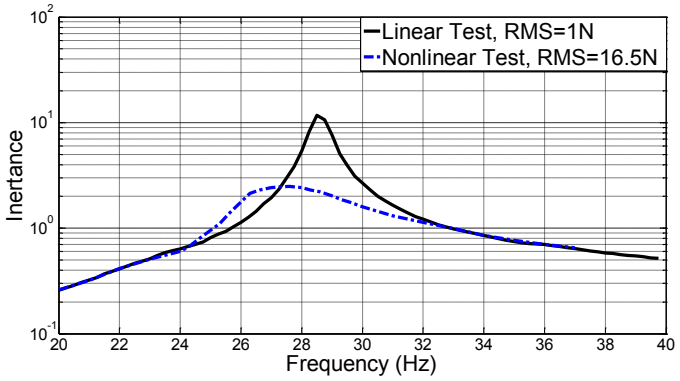

Downloaded from ascelibrary.org by University of Newcastle on 12/17/13. Copyright ASCE. For personal use only; all rights reserved.

Accepted Manuscript
Not Copyedited

Copyright 2013 by the American Society of Civil Engineers

Fig7_b.pdf

Journal of Engineering Mechanics. Submitted April 23, 2013; accepted December 2, 2013;
posted ahead of print December 4, 2013. doi:10.1061/(ASCE)EM.1943-7889.0000759

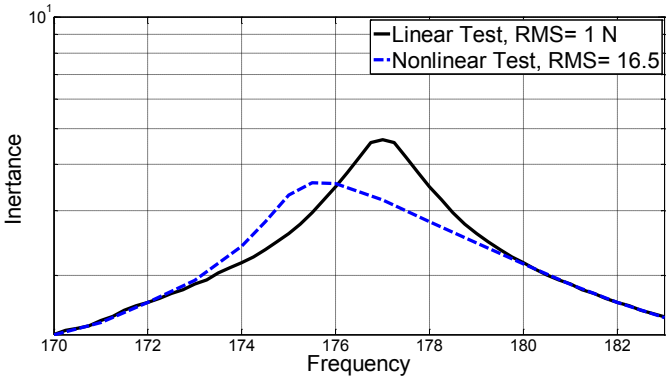

Downloaded from ascelibrary.org by University of Newcastle on 12/17/13. Copyright ASCE. For personal use only; all rights reserved.

Accepted Manuscript
Not Copyedited

Copyright 2013 by the American Society of Civil Engineers

Fig8_a.pdf

Journal of Engineering Mechanics. Submitted April 23, 2013; accepted December 2, 2013;
posted ahead of print December 4, 2013. doi:10.1061/(ASCE)EM.1943-7889.0000759

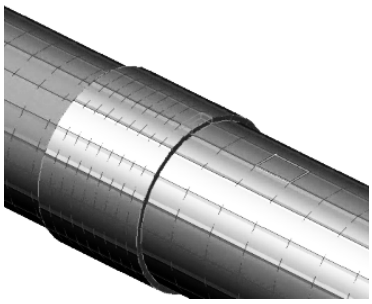

Downloaded from ascelibrary.org by University of Newcastle on 12/17/13. Copyright ASCE. For personal use only; all rights reserved.

Accepted Manuscript
Not Copyedited

Copyright 2013 by the American Society of Civil Engineers

Fig8_b.pdf

Journal of Engineering Mechanics. Submitted April 23, 2013; accepted December 2, 2013;
posted ahead of print December 4, 2013. doi:10.1061/(ASCE)EM.1943-7889.0000759

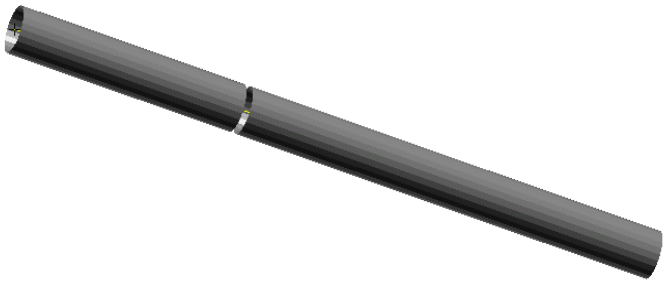

Downloaded from ascelibrary.org by University of Newcastle on 12/17/13. Copyright ASCE. For personal use only; all rights reserved.

Accepted Manuscript
Not Copyedited

Copyright 2013 by the American Society of Civil Engineers

Fig9.pdf

Journal of Engineering Mechanics. Submitted April 23, 2013; accepted December 2, 2013;
posted ahead of print December 4, 2013. doi:10.1061/(ASCE)EM.1943-7889.0000759

Downloaded from ascelibrary.org by University of Newcastle on 12/17/13. Copyright ASCE. For personal use only; all rights reserved.

Accepted Manuscript
Not Copyedited

Copyright 2013 by the American Society of Civil Engineers

Fig10.pdf

Journal of Engineering Mechanics. Submitted April 23, 2013; accepted December 2, 2013;
posted ahead of print December 4, 2013. doi:10.1061/(ASCE)EM.1943-7889.0000759

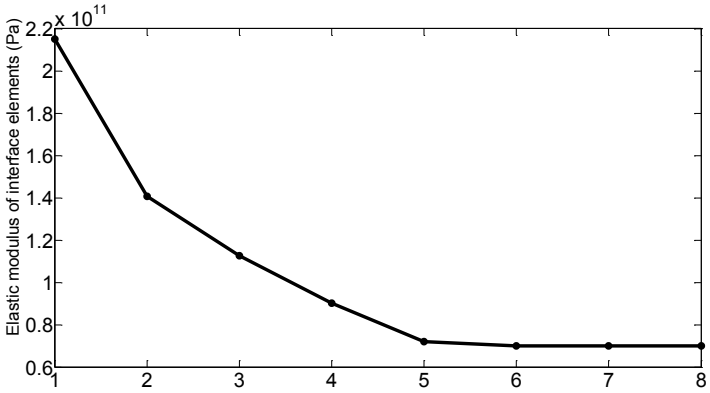

Downloaded from ascelibrary.org by University of Newcastle on 12/17/13. Copyright ASCE. For personal use only; all rights reserved.

Accepted Manuscript
Not Copyedited

Copyright 2013 by the American Society of Civil Engineers

Fig11_a.pdf

Journal of Engineering Mechanics. Submitted April 23, 2013; accepted December 2, 2013;
posted ahead of print December 4, 2013. doi:10.1061/(ASCE)EM.1943-7889.0000759

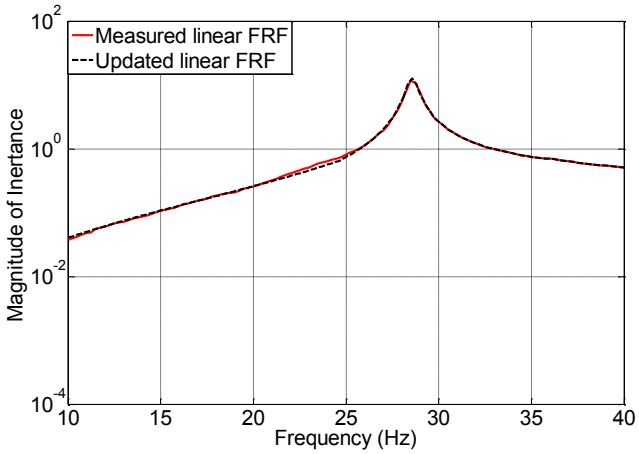

Downloaded from ascelibrary.org by University of Newcastle on 12/17/13. Copyright ASCE. For personal use only; all rights reserved.

Accepted Manuscript
Not Copyedited

Copyright 2013 by the American Society of Civil Engineers

Fig11_b.pdf

Journal of Engineering Mechanics. Submitted April 23, 2013; accepted December 2, 2013;
posted ahead of print December 4, 2013. doi:10.1061/(ASCE)EM.1943-7889.0000759

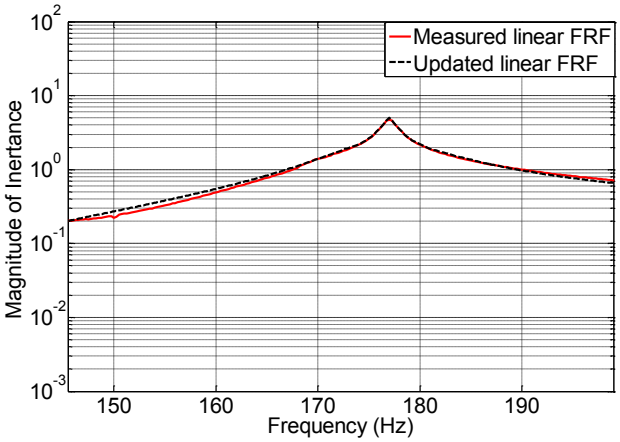

Downloaded from ascelibrary.org by University of Newcastle on 12/17/13. Copyright ASCE. For personal use only; all rights reserved.

Accepted Manuscript
Not Copyedited

Copyright 2013 by the American Society of Civil Engineers

Fig12.pdf

Journal of Engineering Mechanics. Submitted April 23, 2013; accepted December 2, 2013;
posted ahead of print December 4, 2013. doi:10.1061/(ASCE)EM.1943-7889.0000759

Downloaded from ascelibrary.org by University of Newcastle on 12/17/13. Copyright ASCE. For personal use only; all rights reserved.

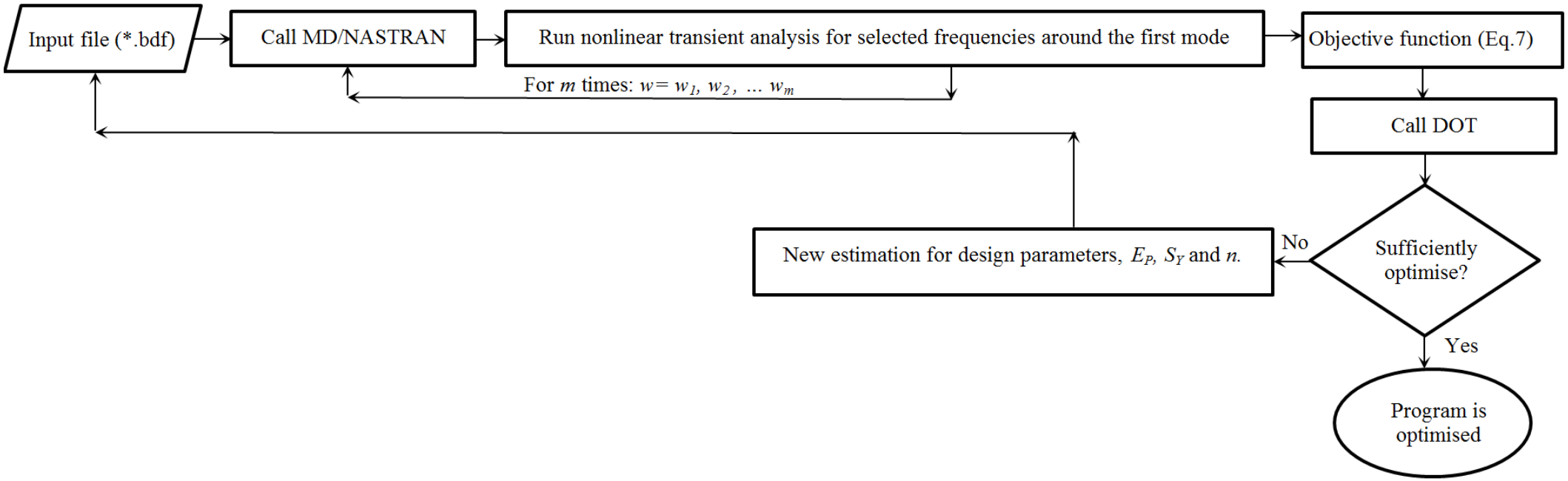

Accepted Manuscript
Not Copyedited

Copyright 2013 by the American Society of Civil Engineers

Fig13.pdf

Journal of Engineering Mechanics. Submitted April 23, 2013; accepted December 2, 2013;
posted ahead of print December 4, 2013. doi:10.1061/(ASCE)EM.1943-7889.0000759

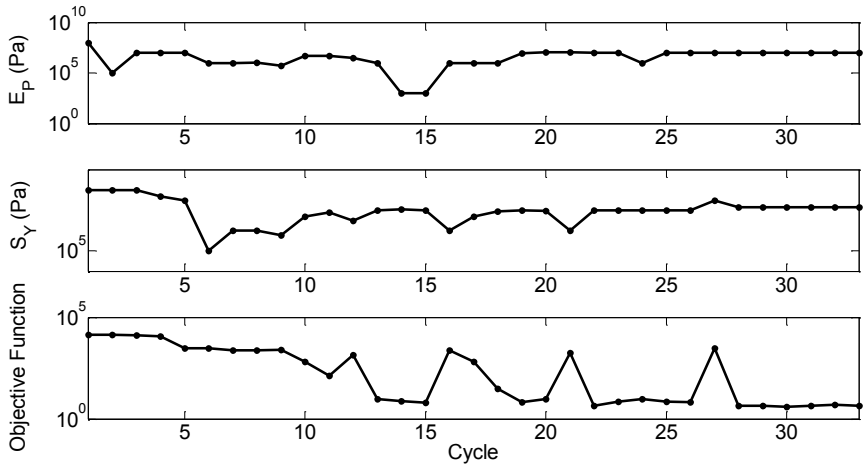

Downloaded from ascelibrary.org by University of Newcastle on 12/17/13. Copyright ASCE. For personal use only; all rights reserved.

Accepted Manuscript
Not Copyedited

Copyright 2013 by the American Society of Civil Engineers

Fig14_a.pdf

Journal of Engineering Mechanics. Submitted April 23, 2013; accepted December 2, 2013;
posted ahead of print December 4, 2013. doi:10.1061/(ASCE)EM.1943-7889.0000759

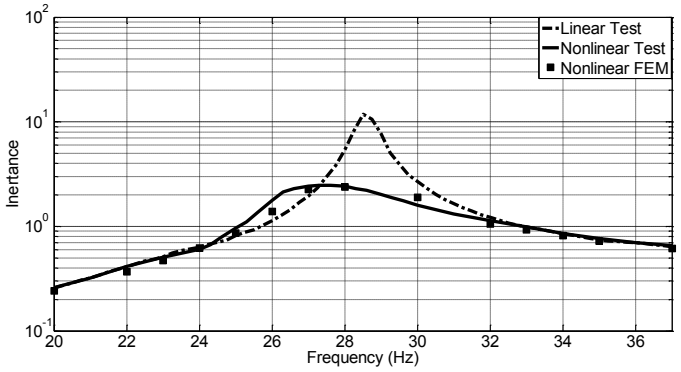

Downloaded from ascelibrary.org by University of Newcastle on 12/17/13. Copyright ASCE. For personal use only; all rights reserved.

Accepted Manuscript
Not Copyedited

Copyright 2013 by the American Society of Civil Engineers

Fig14_b.pdf

Journal of Engineering Mechanics. Submitted April 23, 2013; accepted December 2, 2013;
posted ahead of print December 4, 2013. doi:10.1061/(ASCE)EM.1943-7889.0000759

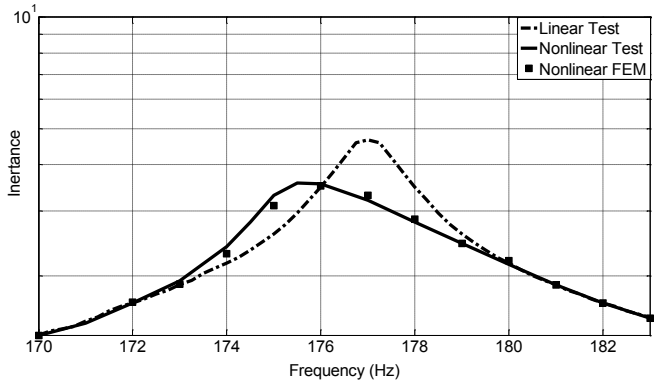

Downloaded from ascelibrary.org by University of Newcastle on 12/17/13. Copyright ASCE. For personal use only; all rights reserved.

Accepted Manuscript
Not Copyedited

Copyright 2013 by the American Society of Civil Engineers

Journal of Engineering Mechanics. Submitted April 23, 2013; accepted December 2, 2013;
posted ahead of print December 4, 2013. doi:10.1061/(ASCE)EM.1943-7889.0000759

Table 1. First four measured natural frequencies (Hz) of the longer pipe in separated free-supported condition.

f_1	f_2	f_3	f_4
568.7	905	940	1070

Table 2. Comparison of the responses between the condensed system and the original one

Number of kept modes	**No reduction**	**5 modes**	**30 modes**
Time (Sec)	357	133	148
Response (m)	5.34e-03	5.29e-3	5.31e-3
Error (%)	---	0.94	0.56

Table 3. Comparison between the measured and predicted natural frequencies before and after updating (Hz)

Mode No.	**Initial model**	**Updated model**	**Test Results**	**Error between initial model and test results (%)**
First Bending Mode (Hz)	32.90	28.49	28.50	15.44
Second Bending Mode (Hz)	203.26	177.00	177.00	14.84

Table 4. Identification of parameters associated with nonlinear portion of the constitutive law

$E_P(Pa)$	$S_Y(Pa)$	n
1.00e7	1.40e7	3.6

Downloaded from ascelibrary.org by University of Newcastle on 12/17/13. Copyright ASCE. For personal use only; all rights reserved.

Accepted Manuscript
Not Copyedited

Copyright 2013 by the American Society of Civil Engineers